Preprints.org

Article

Not peer-reviewed version

Partitioning of Dissolved Organic Carbon, Major Element and Trace Metal During Laboratory Freezing of Organic Leachates From Permafrost Peatlands

Irina S. Ivanova , Liudmila S. Shirokova , Jean-Luc Rols , Oleg S. Pokrovsky *

Posted Date: 13 March 2023

doi: 10.20944/preprints202303.0200.v1

Keywords: peat; freezing; thawing; major; trace elements; organic carbon; experiments

Preprints.org is a free multidiscipline platform providing preprint service that is dedicated to making early versions of research outputs permanently available and citable. Preprints posted at Preprints.org appear in Web of Science, Crossref, Google Scholar, Scilit, Europe PMC.

Copyright: This is an open access article distributed under the Creative Commons Attribution License which permits unrestricted use, distribution, and reproduction in any medium, provided the original work is properly cited.

Preprints (www.preprints.org) | NOT PEER-REVIEWED | Posted: 13 March 2023

doi:10.20944/preprints202303.0200.v1

Disclaimer/Publisher's Note: The statements, opinions, and data contained in all publications are solely those of the individual author(s) and contributor(s) and not of MDPI and/or the editor(s). MDPI and/or the editor(s) disclaim responsibility for any injury to people or property resulting from any ideas, methods, instructions, or products referred to in the content.

Article

Partitioning of Dissolved Organic Carbon, Major Element and Trace Metal During Laboratory Freezing of Organic Leachates From Permafrost Peatlands

Irina S. Ivanova [1], Liudmila S. Shirokova [1,2], Jean-Luc Rols [3] and Oleg S. Pokrovsky [4,5,*]

[1] Tomsk branch of the Trofimuk institute of petroleum geology and geophysics of Siberian branch of the Russian Academy of Sciences, 4 Akademichesky Pr., Tomsk, Russia; IvanovaIS_1986@mail.ru
[2] N. Laverov Federal Center for Integrated Arctic Research of the Ural Branch of the Russian Academy of Sciences, Arkhangelsk, 23 Nab Severnoi Dviny, Russia; lshirocova@yandex.ru
[3] Laboratoire écologie fonctionnelle et environnement, Université de Toulouse, CNRS, Toulouse INP, Université Toulouse 3 – Paul Sabatier (UPS), Toulouse, France; jean-luc.rols@univ-tlse3.fr
[4] BIO-GEO-CLIM Laboratory, Tomsk State University, 35 Lenina Pr., Tomsk, Russia
[5] Geosciences and Environment Toulouse, UMR 5563 CNRS, University of Toulouse, 14 avenue Edouard Belin, 31400 Toulouse, France; oleg.pokrovsky@get.omp.eu
* Correspondence: oleg.pokrovsky@get.omp.eu; Tel.: +33561332625

Featured Application: Elaboration of unified experimental protocol for studying freezing and thawing of organic-rich (humic) natural waters under laboratory conditions

Abstract: The climate change is likely to modify the freezing-thawing cycles in soils and surface waters of permafrost-affected and subarctic regions. Yet, the change of solution chemical composition during ice formation and evolution of remaining fluids remain very poorly known. Towards better understanding of dissolved (< 0.45 µm) organic carbon, major and trace elements behavior in permafrost peatland environments, here we performed laboratory freezing of peat leachates, from complete freezing to complete thawing in order to quantify the partitioning of solutes between the aqueous solution and the remaining ice. We hypothesized the existence of two main groups of solutes, behaving conservatively or non-conservatively during freezing depending on their incorporation into the ice or ability to coagulate in the form of insoluble minerals or amorphous materials in the fluid phase. An unexpected result of this work was that, despite sizable degree of element concentration in the remaining fluid and possible coagulation of organic, organo-mineral and inorganic compounds, the freezing and subsequent thawing produced the final concentrations of most solutes which were not drastically different from initial concentrations in starting leachates, prior freezing. This demonstrates high stability of dissolved (< 0.45 µm) OC, Fe, Al and some trace metals to repetitive freezing and thawing of surface waters in permafrost peatlands.

Keywords: peat; freezing; thawing; major; trace elements; organic carbon; experiments

1. Introduction

The climate warming in high latitudes leads to change of frequency of seasonal thawing-freezing regime [1,2]. However, in contrast to relatively good empirical and modelling understanding of physical aspects of soil freeze/thaw processes [1,3], the behavior of aqueous solutes (< 0.45 µm) upon freezing and thawing of organic matter-rich surface and soil waters of permafrost peatlands remain poorly understood. It is known that both peat porewaters [4,5] and surface waters [6,7] of these regions are strongly enriched in dissolved organic carbon (DOC) and some trace metals. These solutes are often present in the form of organic and organo-mineral colloids [8–10] which are likely to coagulate upon ice formation, for example, during full freezing of surface depressions and shallow thermokarst lakes and ponds [11]. In contrast to sizable number of works devoted to characterizing the impact of freezing and thawing on mineral soil properties [12–30], the freezing/thawing impact

© 2023 by the author(s). Distributed under a Creative Commons CC BY license.

on chemical composition of porewater and ice has not been well described and most often, the researchers have to rely on modelling predictions [31].

Although laboratory experiments allow for identification of governing factors during freezing/thawing effects [32–39], their applications to naturally-relevant aquatic settings of high latitude permafrost peatlands remain very restricted. Previous works in permafrost peatlands reported translocation of microorganisms and changes in porewater chemistry (pH, UV absorbance, dissolved organic carbon (DOC), and major and trace element concentrations) after thawing and bidirectional freezing of the peat core [40,41]. Another recent study examined the impact of freezing/thawing cycles (FTC) on 0.22 µm-filtered waters from North East European permafrost peatland, including leachates of vegetation and soil, as well as natural surface waters [42]. These authors reported only minor (< 5% - 15%) changes of DOC and labile ion concentrations, but several trace elements (Fe, Al, P, Mn, As, and REE) exhibited sizable decrease in concentration after FTC. We therefore hypothesize an overwhelming impact of colloidal status of DOC and trace metal on this coagulation/dissolution processes during freezing and thawing. However, quantitative assessments of these effects are still missing. In the present study, we aimed at 1) elaborating optimal experimental procedure allowing to discrete collection of remaining water during complete freezing progress; 2) quantifying the partitioning coefficients of elements between water and ice and 3) testing the relationship between different elements depending on their speciation and affinity to dissolved organic matter.

We hypothesize the existence of several group of contrasting solutes – 1) those incorporating into forming ice; 2) those remaining in the fluid phase via concentrating due to freezing front migration but not subjected to coagulation, and 3) less soluble complex organo-mineral amorphous compounds or certain minerals, subjected to reversible or irreversible coagulation. Testing these mechanistic hypotheses constituted the first objective of this study. The second objective was to use laboratory leachates of natural substrates (peat) as surrogates for direct experimental modelling of chemical and physical processes occurring in shallow surface waters and topsoil horizons during autumn – spring period. We anticipate that achieving these objectives should allow uniform approach for laboratory modelling of natural aquatic processes in permafrost peatlands and provide useful background for assessing the impact of climate change on chemical composition of surface waters in these environmentally-important regions.

2. Materials and Methods

2.1. Organic substrates from permafrost peatlands used for aqueous leachate preparation

Peat core samples were collected in the end of the summer, in two largest permafrost peatlands of Northern Eurasia – Bolshezemelskaya Tundra (NE Europe) and Western Siberia Lowland. Two peat horizons, thawed (surface, of 0 to 10 cm) and deep (frozen, between 40 and 50 cm) were collected from the center of frozen peat mound about 1 m in diameter. The depth of the active layer on the sampling sites is between 30 and 40 cm, and the permafrost is discontinuous. The dominant vegetation on the mound is mosses and lichens with some dwarf shrubs. The detailed description of environmental context of the sampling sites is provided elsewhere (for Bolshezemelskaya Tundra [43,44] and for western Siberia [45,46]).

To prepare aqueous leachates, 10 g of dry sample (thawed and frozen peat) was reacted at the shaker at 25°C with 1 L of Milli-Q water during 24 h under aerobic conditions, with periodic aeration. The resulted suspension was filtered through sterile single-use Millipore filter unit and placed in broad mouth, PES jars of 150 mL volume.

2.1. Freezing experiments of aqueous leachates

Freezing experiments were conducted in two main setups: with insulation by polyurethane (approximately 10 cm around the jars and the bottom), and without insulation, as illustrated in Figure 1. Inside the plastic jar, we placed a flexible tube which was connected to a syringe and which allowed sampling of fluid in the course of experiment. The freezing occurred from the borders to the center of the jar in case of no-insulated reactors, and from the surface to the bottom in case of insulated reactors (Figure 1). As such, the sampling tube was located at the center of the jar for non-insulated reactors and at the bottom of the jar in case of insulated reactors.

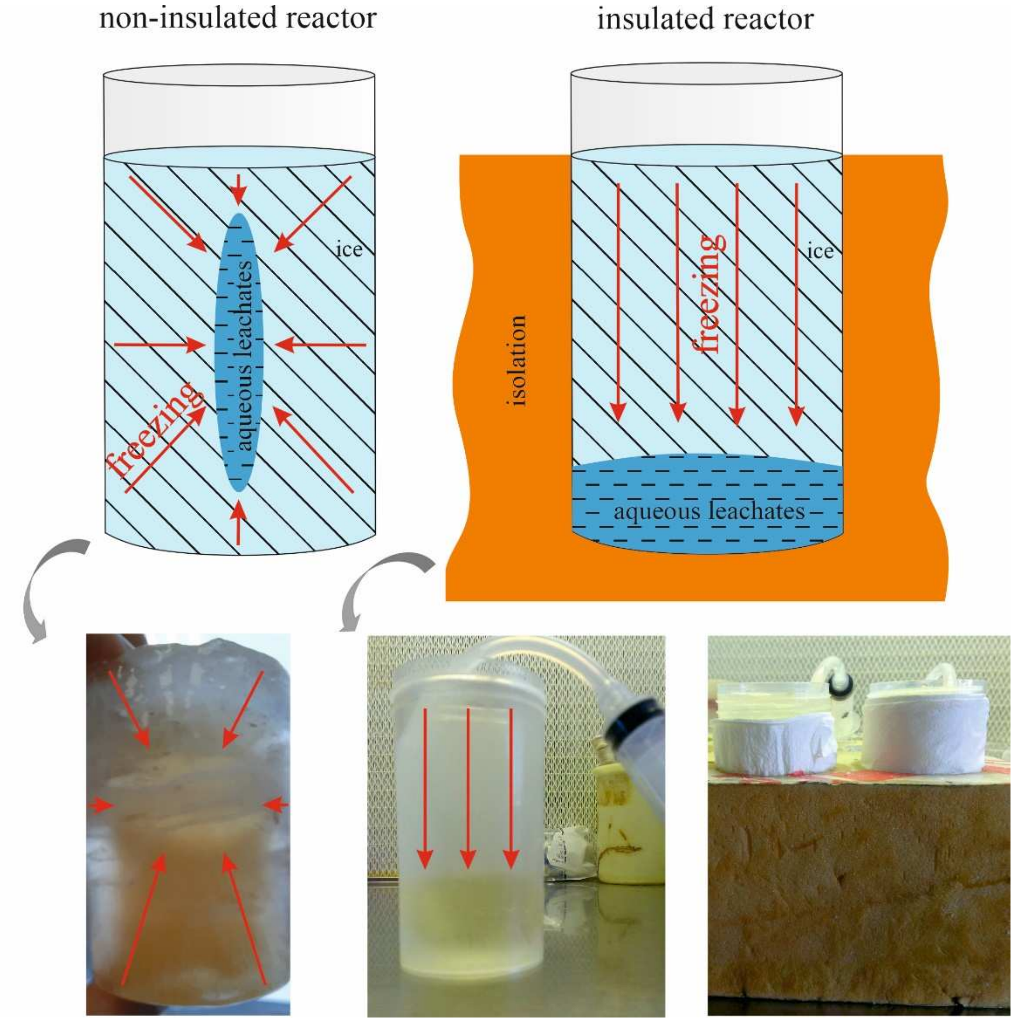

Figure 1. A scheme of experiments and photos of experimental reactors.

Two main type of experiments involved i) progressive freezing, when we started from liquid leachates (filtered < 0.45 µm) and allowed them to freeze at -18 °C, and ii) progressive thawing when, first, we froze solid a series of < 0.45 µm filtered leachates and then we monitored their thawing at room temperature, 20°C. In order to avoid the change of fluid : ice ratio during sampling, we used a single-reactor sacrificial sampling technique. For this, instead of consecutive sampling from the same reactor, 10 identical reactors with filtered leachates were prepared simultaneously and placed in the freezer. Each sampling used the entire reactor which was then removed from the freezer and discarded.

The sampling was performed regularly as following. Samples of aqueous leachate of peats with insulant were taken after 6, 8, 11, 15 hours, whereas samples of aqueous leachate of peat BZT were taken after 6, 11, 29, 31 hours. Samples of aqueous leachate of peats without insulant were taken after 4, 5, 6 hours, and samples of aqueous leachate of peat BZT were taken after 4, 5 hours. During unfreezing of aqueous leachate of WSL peat, samples were collected after 2, 3, 6 hours, samples of aqueous leachate of peat BZT were collected after 1, 2, 3, 5, 7 hours. Typically, between 30 and 50% of the remaining or formed fluid was collected; the volume of sampled fluid did not exceed 15 % of the initial volume. Immediately before sampling, the reactors were vigorously shaken to homogenize the precipitate that could have been formed in the remaining fluid. This allowed avoiding the dilution or concentration of solutes relative to precipitates formed during freezing of peat leachates.

2.3. Chemical analyses

A non-filtered subsample of the fluid which was extracted from freezing reactor was used to measure pH (uncertainty of ± 0.01 pH units) and specific conductivity (± 0.1 µS cm^{-1}). The rest of the 15 mL was filtered through a 0.45 µm Minisart® syringe filter. In the < 0.45 µm filtrates, the DOC and DIC were analyzed by high-temperature catalytic oxidation using TOC-VCSN, Shimadzu® (uncertainty ± 2%, 0.1 mg L^{-1} detection limit). The DIC was measured after sample acidification with HCl and DOC was analyzed in acidified samples after sparging it with C-free air for 3 min at 100 mL min-1 as non-purgable organic carbon (NPOC). The internationally certified water samples (MISSISSIPPI-03, Pérade-20) were used to check the validity and reproducibility of the analysis. The UV-absorbance of water samples was measured using a 10 mm quartz cuvette on a CARY-50 UV-vis spectrophotometer to assess the aromaticity of pore fluids via specific UV absorbance ($SUVA_{254}$). Major cations, Si, P and ~40 trace elements (TE) were measured with a quadrupole ICP-MS (Agilent 7500 ce) using In and Re as internal standards. The international geo-standard SLRS-5 (Riverine Water Reference Material for Trace Metals) was used to check validity and the quality control of analyses [47,48].

2.4. Data interpretation

In order to identify the group of solutes depending on their partitioning between the forming ice and the remaining solution, we normalized the concentration of main non–conservative solutes (DOC, Fe, Al, P, Mn, Sr, trivalent and tetravalent hydrolysates) to that of major and inert components, not subjected to coagulation/mineral precipitation such as K, Na, or Cl. Note that we could not use Mg, Ca, Si and sulfate for such a normalization, because these ions can form sparingly soluble salts (Mg, Ca carbonates, Ca sulfate, Mg hydrous silicate) upon progressive concentration of the remaining fluid during freezing. Assuming that there is no (or very little) incorporation of soluble labile ions into the ice structure, we calculated, at each time (t) the degree of element accumulation in the remaining fluid relative to the initial concentration, i.e., element concentration factor (F_{conc}) as following:

$$F_{conc} = C_t/C_0, \qquad (1)$$

To differentiate between conservative and non-conservative elements, the F_{conc} value of each element at each time t of sampling was normalized to that of Na and traced as a function of time, for each consecutive sampling.

Besides, in order to better differentiate between groups of elements, we performed pairwise (Pearson) correlations between elements in the fluid phase, considering all substrates and all types of treatments together. Significance criterion was set at $p < 0.05$. Significance of the difference in element concentration between different experimental treatments (freezing and thawing; with and without isolation; surface and deep peat horizon; peat from NE European tundra and western Siberia) was examined by pairwise Mann-Whitney test at $p < 0.05$.

3. Results

3.1. Initial leachate composition and the impact of reactor design and freezing mode on element concentration in the remaining fluid

There were significant differences in element concentrations in the initial leachate of frozen and thawed peat horizons, as well as between the peat of NE European tundra (BZT) and Western Siberia (WSL). Thus, the leachates of peat from the NE European Tundra demonstrated sizably lower pH than those of the WSL (4.75 and 6.0±0.25, respectively), and 2.5 times higher DOC concentration (Table 1).

Table 1. Element concentrations in the initial leachate (< 0.45 µm) of frozen peat from NE European tundra (BZT) and frozen and thawed peat horizons of Western Siberia (F WSL and WSL, respectively).

Element	Western Siberia Lowland		European tundra	Element	Western Siberia Lowland		European tundra
	WSL	F WSL	BZT		WSL	F WSL	BZT
UV_{245}, nm	0.386	0.167	1.037	Zr, µg/L	0.0192	0.0878	0.4806
pH	5.78	6.2	4.74	Nb, µg/L	0.0015	0.0007	0.0095
DOC, mg/L	9.1	8.0	27.4	Mo, µg/L	0.1083	0.9193	0.034
Li, µg/L	0.01	0.01	NA	Cd, µg/L	0.0607	0.0579	0.0045
B, µg/L	59.2	54.8	72.3	Sb, µg/L	0.0144	0.0566	0.007
Na, µg/L	915	686	1472	Cs, µg/L	0.0004	0.0004	0.0015
Mg, µg/L	73	8	150.3	Ba, µg/L	163.8	10.56	245
Al, µg/L	15.6	9.8	78.1	La, µg/L	0.0214	0.0137	0.0375
Si, µg/L	32	19	388	Ce, µg/L	0.032	0.0277	0.069
P, µg/L	9.2	15.0	68.3	Pr, µg/L	0.0031	0.0024	0.0084
K, µg/L	215	113.3	732.5	Nd, µg/L	0.0141	0.0096	0.0362
Ca, µg/L	289	257.3	571.7	Sm, µg/L	0.0049	0.0017	0.0101
Ti, µg/L	0.106	0.1155	0.439	Eu, µg/L	0.0119	0.0011	0.0192
V, µg/L	0.360	0.2248	0.176	Gd, µg/L	0.0054	0.0031	0.0147
Cr, µg/L	0.040	0.06	0.460	Tb, µg/L	0.0005	0.0003	0.0017
Mn, µg/L	1.26	0.1153	0.0323	Dy, µg/L	0.004	0.0023	0.0095
Fe, µg/L	22.9	12.3	56.0	Ho, µg/L	0.0007	0.0003	0.0017
Co, µg/L	0.015	0.0104	0.0373	Er, µg/L	0.0068	0.0047	0.0058
Ni, µg/L	0.17	0.18	0.26	Tm, µg/L	0.0005	0.0001	0.0009
Cu, µg/L	0.674	0.7167	25.4	Yb, µg/L	0.0024	0.0009	0.0059
Zn, µg/L	212	8.62	420	Lu, µg/L	0.0003	0.0002	0.0008
Ga, µg/L	0.0002	0.0006	0.0181	Hf, µg/L	0.0019	0.0089	0.0343
As, µg/L	0.1754	0.1352	0.2781	W, µg/L	0.0069	0.0558	0.005
Rb, µg/L	0.08	0.05	0.26	Pb, µg/L	0.044	0.025	1.406
Sr, µg/L	4.96	2.417	5.048	Th, µg/L	0.0019	0.0017	0.0204
Y, µg/L	0.0248	0.0114	0.0514	U, µg/L	0.0013	0.003	0.0074

As a result of such high acidity of organic-rich waters, the leachates of BZT peat were sizably, by a factor of 2 to 3, richer in Fe, Al, and other trace metals compared to those from the WSL peat. The leachates from active horizon of the WSL peat layer exhibited 0.4 unit lower pH values, 1.5 to 2.0

Preprints (www.preprints.org) | NOT PEER-REVIEWED | Posted: 13 March 2023 doi:10.20944/preprints202303.0200.v1

times higher concentrations of Si, K, Fe, Al, Sr and 10-20 times higher Mn, Zn, and Ba than the leachates from the frozen peat horizons.

3.2. Evolution of pH, DOC and metal concentration in the fluid phase during freezing and thawing of peat leachates

Preliminary examination of the concentration evolution in the course of freezing and thawing (two directions) demonstrated that there was no significant (at $p < 0.05$) difference between two treatments in terms of pH, DOC, major and trace element concentration evolution. Progressive freezing of aqueous peat leachates led to a decrease in pH relative to the initial solutions (Figure 2), and a general increase in DOC and element concentrations, but this increase was different among peat samples. Thus, sizable, a factor of 2 to 3, increase in concentration of most elements in the remaining fluid occurred during freezing of leachates from active (upper) layer peat of both Western Siberia (WSL) and NE European Tundra (BZT), shown as brown and black symbols, respectively, in Figure 2.

This was not the case for the leachates of frozen Siberian peat: this sample did not exhibit any systematic change in concentration of solutes during progressive freezing and thawing (shown by blue symbols in Figure 2). Such a drastic difference in the behavior of leachates from frozen and thawed peat horizons is not linked to pH or DOC behavior but likely to be intrinsic properties of leachates, which depended on the position of the peat sample at the core with respect to active layer depth.

Progressive thawing of completely frozen leachates produced a decrease in concentration after each subsequent sampling (shown as crosses in Figure 2); the curve approximating element concentration versus time followed approximately the one of progressive freezing. This was observed for most analyzed elements, including DOC, Fe, Al, P, some divalent trace metals, trivalent and tetravalent hydrolysates.

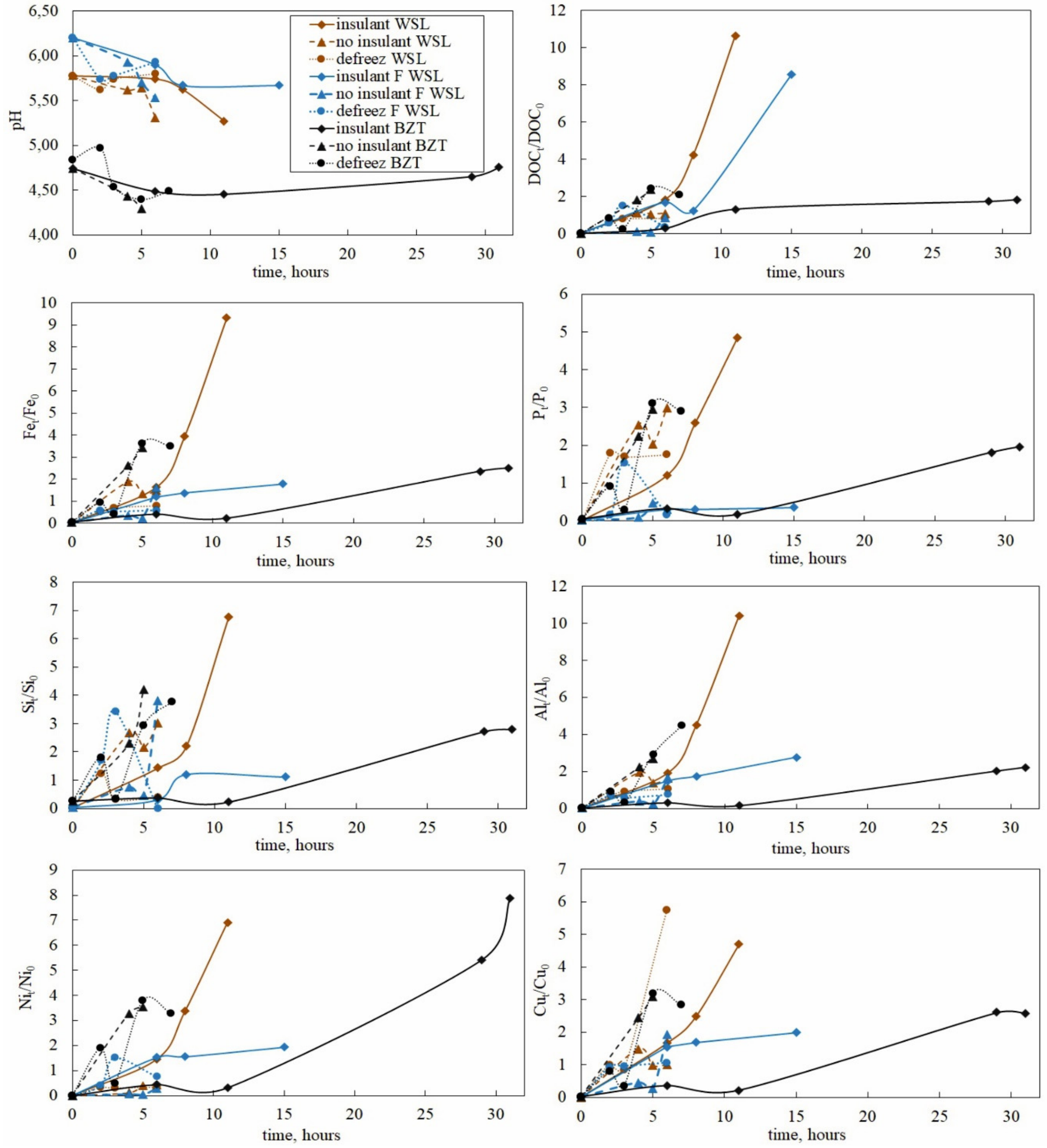

Figure 2. Temporal evolution of pH and solute (DOC, Fe, P, Si, Al, Ni and Cu) concentrations in the remaining and forming fluid during progressive freezing and thawing, respectively, of peat leachates obtained from active (thawed) and permanently frozen (below active layer depth) peat horizons of permafrost peatlands in Northern Eurasia. Freezing is shown by diamonds and triangles whereas thawing is shown by circles. The concentration of element at time t and initial (0) were normalized to that of sodium. Connecting lines are for guiding purposes.

We found that the initial concentration of some elements in leachates (prior) freezing were not always recovered after full freezing and thawing of the reactors (Figure 3). This result is consistent with previous works on freezing/thawing cycles of filtrates from northern peatlands that demonstrated sizable coagulation and removal of low-soluble elements, bound to organic colloids [42,49].

Preprints (www.preprints.org) | NOT PEER-REVIEWED | Posted: 13 March 2023 doi:10.20944/preprints202303.0200.v1

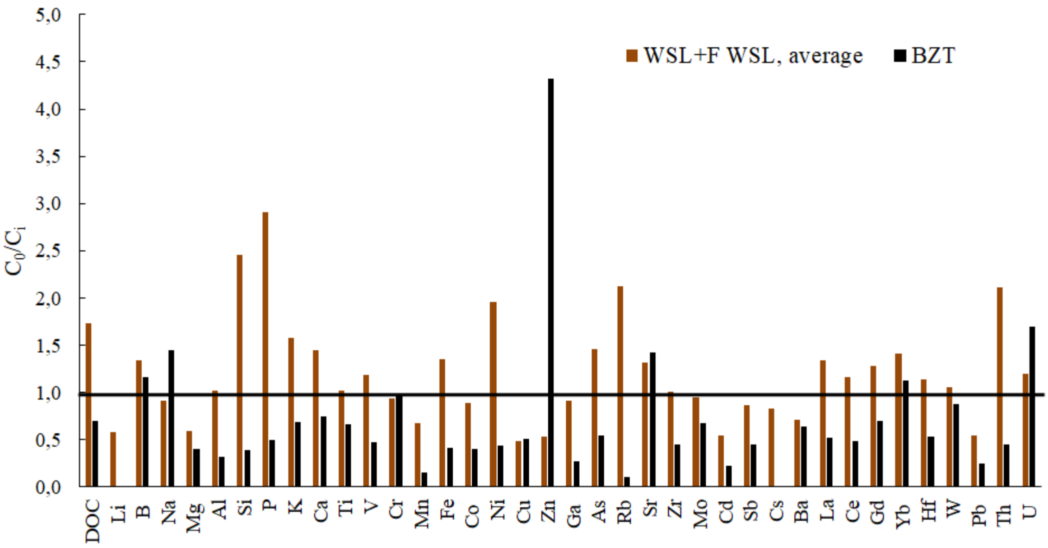

Figure 3. A histogram of ratios of element concentration in the leachate prior to freezing (C_0) to the final concentration after entire freezing/thawing cycle. The values above 1 indicate some removal of an element in the form of coagulates. The values below 1 likely represent experimental / analytical artifacts.

Considering the element recovery upon entire freezing/thawing cycle, three group of elements, separately for each substrate, could be distinguished (Table 2).

Table 2. Degree of element recovery during entire reversible freezing and thawing cycle, separately for < 0.45 µm leachates of peat from BZT, and from frozen (F WSL) and thawed (WSL).

WSL	F WSL	BZT
	C_0/C_{final} <0.5	
Li, Cu, Pb , Th, U	Mg, Mn, Zn, Cd, Ba	Mg, Al, Si, V, Mn, Fe, Co, Ni, Ga, Rb, Zr, Cd, Sb, Cs, Ce, Pb, Th
	C_0/C_{final} 0.5–1.5	
DOC, B, Na, Mg, Al, P, K, Ca, Ti, V, Cr, Mn, Fe, Co, Zn, Ga, As, Rb, Sr, Zr, Mo, Cd, Sb, Cs, Ba, REEs, Hf	Li, B, Na, Al, Ti, V, Fe, Co, Ni, Cu, Ga, Zr, Mo, Sb, Cs, Ba, REEs, Hf, Pb, U	DOC, B, Na, P, K, Ca, Ti, Cr, Cu, As, Sr, Mo, Ba, REEs, Hf, W
	C_0/C_{final} 1.5–3	
Si, Ni, Yb	DOC, K, Ca, As, Sr	U
	C_0/C_{final} >3	
	P, Rb, Th	Zn

We discovered that the leachates from frozen peat horizons (WSL) behaved differently from the leachates of thawed horizons; namely, in the case of leachate of frozen peat, the element concentration in the remaining fluid during progressive freezing did not increase significantly, and remained rather constant over time. This contrasted the temporal pattern of thawed peat leachates: the concentration of elements in the remaining fluid strongly increased upon freezing (Figure 2). This result could signify efficient incorporation of solutes from frozen peat leachates into the forming ice, as reflected by quite low partitioning coefficients of elements between forming ice and remaining fluid, for this

Preprints (www.preprints.org) | NOT PEER-REVIEWED | Posted: 13 March 2023 doi:10.20944/preprints202303.0200.v1

type of substrate. We have no explanation for potential mechanism of rather unexpected behavior of this particular leachate but we can hypothesize that some volumes of the fluid, formed from frozen leachate, partially preserved the peat dispersed ice structure and chemical composition (i.e., [9,50]) and could be directly incorporated into forming ice with a partitioning coefficient close to 1. Clearly, further freezing/thawing experiments, including assessment of colloidal forms of aquatic leachates obtained from permanently frozen peat horizons (sampled below the active layer boundary) are needed to verify and develop this hypothesis.

3.3. Group of elements depending on their conservative and non-conservative behavior during freezing revealed via correlation relationships

The correlations between element concentrations during freezing and thawing at different modes (with and without insulant, Figure 4 and Table 3) allowed distinguishing two main groups of solutes: DOC, Fe, Al as potential carries of Si, P, K, Cr, Co, Ni, Cu, As, Pb, Nb and trivalent and tetravalent hydrolysates and Ca, Na, K as major indicators of conservative solutes which did not exhibit any significant correlations with other solutes. It was found that, while Fe, Al, other trace metals notably TE^{3+}, TE^{4+}, exhibited strong correlations during freezing and thawing, the labile Na or Ca (as major cation) did not correlate with Fe, Al and DOC in none of the substrates. Note that maximal number of elements correlated with three major components of organo-mineral colloids (DOC, Fe, and Al) was observed in experiments of thawing rather than freezing.

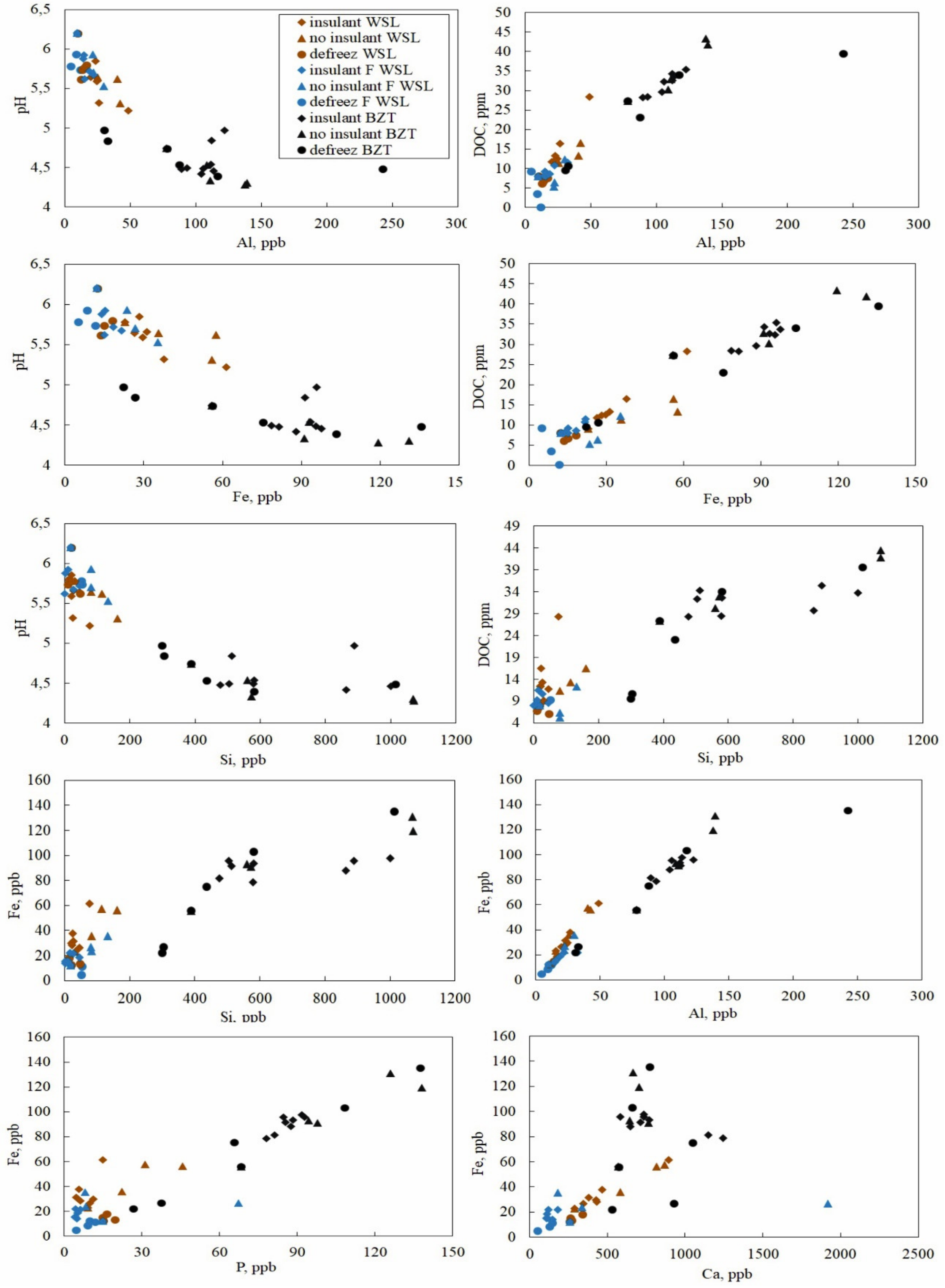

Figure 4. Examples of correlations between solute concentrations for all conducted experiments.

Preprints (www.preprints.org) | NOT PEER-REVIEWED | Posted: 13 March 2023 doi:10.20944/preprints202303.0200.v1

Table 3. Matrix correlation (Pearson, $p < 0.05$ significance level, labelled by asterisk) of element concentration in aqueous solution during freezing (left) and thawing (right) of peat leachates. Experiments with and without insulant are combined together.

	freezing	**WSL+F WSL+BZT**				**thawing WSL+F WSL+BZT**			
	DOC	**Na**	**Al**	**Fe**		**DOC**	**Na**	**Al**	**Fe**
DOC	1	-0.0584	0.9752*	0.9537*	DOC	1	0.1815	0.9320*	0.9695*
Li	0.2841	0.6957	0.4028	0.4249	Li	0.9149*	0.3597	0.9141*	0.9396*
B	0.0137	0.9399*	0.0984	0.1099	B	0.2050	0.9889*	0.1702	0.2581
Na	-0.0584	1	0.0585	0.0556	Na	-0.4262	1	0.1483	0.2255
Mg	0.2708	0.7249*	0.3661	0.3465	Mg	0.6507	0.5771	0.6468	0.6935
Al	0.9752*	0.0585	1	0.9714*	Al	0.9320*	0.1483	1	0.9684*
Si	0.9433*	0.0777	0.9784*	0.9533*	Si	0.9302*	0.2209	0.9686*	0.9516*
P	0.8843*	0.2769	0.9342*	0.9110*	P	0.9797*	0.1920	0.9584*	0.9802*
K	0.8286*	0.0625	0.8723*	0.8240*	K	0.8810*	0.1027	0.9076*	0.8650*
Ca	0.2949	0.7511*	0.3536	0.4123	Ca	0.6472	0.7605*	0.6221	0.6901
Ti	0.9329*	0.1386	0.9767*	0.9448*	Ti	0.9463*	0.3545	0.8872*	0.9503*
V	-0.0965	-0.0566	-0.1673	0.0424	V	0.2062	-0.0739	0.2954	0.3317
Cr	0.7382*	-0.0688	0.7430*	0.6332	Cr	0.8028*	0.5378	0.7283*	0.7761*
Mn	-0.3950	-0.2971	-0.4310	-0.3443	Mn	-0.4973	-0.2645	-0.3969	-0.4086
Fe	0.9537*	0.0556	0.9714*	1	Fe	0.9695*	0.2254	0.9684*	1
Co	0.5802	0.2920	0.6675	0.6908	Co	0.8884*	0.1750	0.9240*	0.9248*
Ni	0.7402*	-0.1376	0.7681*	0.7031*	Ni	0.9220*	0.2549	0.9012*	0.9375*
Cu	0.9422*	0.0668	0.9787*	0.9200*	Cu	0.9824*	0.2509	0.9490*	0.9864*
Zn	0.3588	0.3950	0.3647	0.3455	Zn	0.2217	0.8124*	0.1310	0.2148
Ga	0.9447*	-0.0082	0.9617*	0.8982*	Ga	0.8970*	0.1903	0.9884*	0.9363*
As	0.7844*	-0.0093	0.7550*	0.8698*	As	0.9210*	0.2233	0.9128*	0.9598*
Rb	0.7832*	-0.1507	0.8052*	0.7907*	Rb	0.7769*	-0.1060	0.9331*	0.8367*
Sr	-0.1877	0.5511	-0.1361	-0.0676	Sr	-0.0097	-0.1975	-0.0006	-0.0246
Y	0.8549*	0.0521	0.8609*	0.8934*	Y	0.9522*	0.3111	0.9301*	0.9605*
Zr	0.8053*	0.0260	0.8602*	0.7922*	Zr	0.9661*	0.2834	0.9565*	0.9804*
Nb	0.9546*	0.1243	0.9925*	0.9635*	Nb	0.9577*	0.3725	0.8911*	0.9628*
Mo	-0.5612	0.2892	-0.4798	-0.5046	Mo	-0.4110	-0.2568	-0.3710	-0.4251
Cd	-0.3985	-0.1202	-0.3732	-0.3835	Cd	-0.5188	-0.3213	-0.4304	-0.4827
Sb	-0.5286	0.1542	-0.4595	-0.4747	Sb	-0.3971	-0.2852	-0.3401	-0.3979
Cs	0.6519	-0.1790	0.6329	0.6351	Cs	0.6829	-0.0942	0.8846*	0.7569*
Ba	0.4225	-0.1811	0.4279	0.4552	Ba	0.7095*	-0.0895	0.7918*	0.7180*
La	0.6586	-0.0468	0.6731	0.6531	La	0.9526*	0.1168	0.9755*	0.9722*
Ce	0.6706	-0.0138	0.6699	0.6963	Ce	0.9631*	0.1622	0.9812*	0.9906*
Nd	0.9474*	0.0619	0.9602*	0.9655*	Nd	0.9643*	0.2661	0.9659*	0.9818*
Hf	0.7619*	0.0501	0.8238*	0.7434*	Hf	0.9608*	0.3444	0.9306*	0.9613*
Pb	0.9462*	0.0543	0.9799*	0.9318*	Pb	0.9271*	0.1359	0.9964*	0.9687*
Th	0.9580*	0.0672	0.9842*	0.9479*	Th	0.9781*	0.1818	0.9742*	0.9873*
U	0.3306	0.4467	0.3885	0.3045	U	0.6095	0.5018	0.4967	0.5296

Further insights on group of elemental patterns during freezing and thawing were obtained via consideration of correlations between element distribution factors (K_d solution / ice) as listed in Table 4. These correlations generally confirmed the group of elements described above – non conservative such as DOC, Fe, Al, trace metals, notably trivalent and tetravalent hydrolysates, and conservative major cations (Na, Ca, Mg) and some anions (B). Overall, the number of significant correlations for Kd values was lower than that for concentration values. and the maximal number of inter-correlated elements was observed in thawing experiments.

Table 4. Matrix correlation (Pearson, $p < 0.05$ significance level, labelled by asterisk) of element distribution coefficient (*Kd*) between aqueous solution and ice during freezing (left) and thawing (right) of peat leachates. Experiments with and without insulant are combined together.

freezing WSL+F WSL+BZT (insulant+no insulant)						**thawing WSL+F WSL+ BZT**					
	DOC	**Na**	**Al**	**Ca**	**Fe**		**DOC**	**Na**	**Al**	**Ca**	**Fe**
DOC	1	-0.4156	0.5072	0.0843	0.5100	DOC	1	-0.3016	0.5712	0.1688	0.6304
Li	-0.1530	0.7967*	0.4767	0.7761*	0.4696	Li	0.2761	-0.0676	0.4645	0.3155	0.3766
B	-0.0739	0.6382	0.0415	0.6214	0.1158	B	-0.0679	0.9436*	-0.0395	0.7411*	0.1240
Na	-0.4156	1	0.1041	0.7425*	0.1953	Na	-0.3016	1	-0.1697	0.5711	-0.0609
Mg	-0.2679	0.8074*	0.1838	0.7995*	0.1953	Mg	-0.2314	-0.0126	-0.1526	-0.7061	-0.2045
Al	0.5072	0.1041	1	0.2329	0.7560*	Al	0.5712	-0.1697	1	0.2742	0.9317*
Si	0.1082	0.4472	0.5676	0.3854	0.8156*	Si	0.2021	-0.1342	0.4378	-0.4496	0.3752
P	0.1482	0.4320	0.2525	0.7756*	0.5143	P	0.7269*	-0.3039	0.4626	0.2122	0.4140
K	-0.0056	0.3047	0.6187	0.2150	0.4870	K	-0.2479	-0.0247	0.3868	-0.2146	0.2404
Ca	0.0843	0.7425*	0.2329	1	0.3776	Ca	0.1688	0.5711	0.2742	1	0.4163
Ti	0.5325	0.1927	0.7393*	0.3701	0.8923*	Ti	0.4915	-0.0464	0.7842*	0.4037	0.8648*
V	0.7352*	-0.1233	0.4677	0.3208	0.7364*	V	0.5676	0.0204	0.8124*	0.6671	0.9248*
Cr	0.3214	-0.2685	0.3539	-0.1761	-0.1111	Cr	0.1342	0.0799	0.0982	0.2944	0.0721
Mn	-0.0527	-0.1320	0.4663	-0.3944	0.1574	Mn	-0.2300	0.4363	0.4854	0.2417	0.5073
Fe	0.5100	0.1953	0.7560*	0.3776	1	Fe	0.6304	-0.0609	0.9317*	0.4163	1
Co	0.0272	0.4662	0.7655*	0.2426	0.5674	Co	-0.1855	0.0481	0.5476	-0.0876	0.4929
Ni	0.0342	-0.3260	-0.2851	-0.2410	-0.0968	Ni	0.6660	-0.0068	0.6953	0.3143	0.8425*
Cu	-0.1651	0.3935	0.5024	0.1072	0.6297	Cu	0.2010	-0.1413	0.2787	0.1113	0.1933
Zn	-0.1390	0.0970	0.2811	-0.2016	0.1828	Zn	-0.4330	0.1063	-0.1833	-0.6541	-0.2768
Ga	0.5550	-0.2729	0.4173	0.0082	0.0492	Ga	0.5962	-0.2789	0.5572	-0.0347	0.4060
As	0.7066*	-0.0685	0.3519	0.3874	0.6971	As	0.5922	-0.0274	0.8507*	0.5036	0.8904*
Rb	0.2731	-0.1322	0.6126	-0.0054	0.3259	Rb	0.5634	-0.3121	0.9508*	0.1782	0.8402*
Sr	-0.1735	0.7653*	0.2376	0.8512*	0.2824	Sr	-0.2950	-0.0756	0.1700	-0.3811	-0.0417
Y	0.1877	0.1517	0.5959	0.1345	0.6976	Y	0.5229	0.0566	0.9368*	0.3604	0.9358*
Zr	0.3338	-0.0874	0.4281	0.0913	0.3792	Zr	0.6300	-0.0906	0.9480*	0.4148	0.9705*
Nb	0.0318	0.5789	0.7029*	0.4167	0.7073*	Nb	0.0933	0.1119	0.6551	0.0888	0.7199*
Mo	0.5238	0.2488	0.9165*	0.4235	0.8317*	Mo	0.0401	0.1440	0.6823	0.0976	0.6416
Cd	-0.0607	-0.1219	0.4597	-0.3656	0.2252	Cd	0.2183	-0.1742	0.8165*	0.0156	0.8099*
Sb	0.3598	-0.0489	0.4976	0.1477	0.5904	Sb	0.1665	-0.1549	0.5969	-0.0309	0.4949
Cs	0.5773	-0.2419	0.5398	0.0382	0.3247	Cs	0.5899	-0.2591	0.9123*	0.2353	0.7915*
Ba	-0.2300	0.0473	0.1627	-0.2749	0.0073	Ba	-0.3542	-0.0635	0.0718	-0.6617	-0.0606
La	-0.0399	-0.1035	-0.2501	-0.1054	-0.1870	La	0.5587	-0.1475	0.9793*	0.2546	0.9591*
Ce	0.1158	-0.0381	0.0226	0.0197	-0.0057	Ce	0.6383	-0.1569	0.9644*	0.3963	0.9670*
Pr	0.2602	-0.0751	0.1179	0.0857	0.1968	Pr	0.6663	-0.0715	0.9459*	0.4638	0.9769*
Nd	0.3362	0.0534	0.2615	0.2513	0.4887	Nd	0.6476	-0.0423	0.9222*	0.5276	0.9306*
Sm	0.4565	-0.1096	0.7472*	-0.0797	0.6653	Sm	0.5272	0.0892	0.8231*	0.3027	0.8126*
Gd	0.2701	-0.0438	0.4191	0.0736	0.4928	Gd	0.5253	-0.2441	0.9277*	0.2001	0.8383*
Dy	0.3761	0.0351	0.4851	0.1995	0.7265*	Dy	0.4651	0.0003	0.8763*	0.2797	0.9322*
Yb	0.2059	0.1526	0.5809	0.1827	0.5640	Yb	0.2427	0.2509	0.6487	0.2005	0.6722
Hf	0.2560	-0.0663	0.4668	0.0583	0.2919	Hf	0.5711	0.0393	0.8259*	0.3117	0.8759*
W	-0.0986	0.4389	-0.0700	0.4516	0.0428	W	-0.3747	0.7092*	0.1301	0.3248	0.1942
Pb	-0.1740	0.1610	0.4887	-0.1852	0.2997	Pb	0.4775	-0.2282	0.8482*	0.1417	0.7263*
Th	0.6065	0.1494	0.5774	0.5807	0.7874*	Th	0.5951	-0.1594	0.9138*	0.4679	0.9234*
U	0.2473	0.2469	0.6766	0.3174	0.5078	U	-0.2065	0.3369	0.1920	-0.0993	0.0739

4. Discussion

During freezing of natural porewaters that present in the permafrost peatlands, the solutes are known to be excluded downwards during the autumn freeze-up, when the freezing front propagates from the surface to the bottom of the peat profile [51,52]. During this process, the solutes can be accumulated by a factor of ten to hundreds times in the remaining unfrozen part of the porewaters in mineral and organic soils [51,53,54]. The basic mechanism of DOC and inorganic solutes accumulation in the residual fluid during ice formation in the reactor is simply physically-induced increase in their concentration at the freezing front propagation [55,56]. Numerous experiments on homogeneous and heterogeneous aqueous - solid systems demonstrated that the impurities (present in the form of soluble salts or suspended materials) are separated from aqueous solution by so called dynamic freezing front [57,58]. Other experiments on freezing of natural surface waters of Arctic peatlands similar to peat porewater of the current study demonstrated a progressive freezing of water from reactor edges to the center accompanied by relative accumulation of DOM in the remaining liquid [42,49].

The temporal concentration patterns and elemental correlations demonstrated two contrasting group of solutes - labile elements present in essentially ionic form (alkalis, alkaline-earth metals, oxyanions and neutral molecules) which did not correlate with DOC, Fe and Al and exhibited rather similar correlations in the fluid prior to freezing and after the entire freeze-thaw sequence. Contrasting to these soluble and labile solutes were divalent metals and insoluble TE^{3+}, TE^{4+} trace elements which are known to be carried in the form of organic and organo-mineral (Fe, Al) colloids in the peat porewater (i.e., [10]) and dispersed ice of the peat cores [9]. Therefore, in agreement with previous studies of experimental bi-directional freezing of the entire peat cores (i.e., [40,41], we hypothesize that, during freezing front propagation, large size organic-Fe-Al colloids are subjected to preferential exclusion relative to truly dissolved (inorganic) solutes from the ice. As a result, they form precipitates either in the bulk of remaining fluid or at the very interface between forming ice and remaining aqueous solution.

It is known that high DOM concentration diminish the proportion of DOC incorporated into the ice phase [16,59,60]. In the present study, we observed a positive correlation ($R = 0.94$, $p < 0.01$) between the initial DOC concentration in the leachates and the K_d value of DOC. Note however, that rather high concentration of initial DOM and fast freezing rate (at -20 °C) could drive some parts of ionic solutes and even organic colloids to be occluded in the bulk of forming ice in the form of liquid pockets, as it is known for sea ice formation [61], and has been recently demonstrated for mineral soils [62,63].

Some decrease of DOM between the initial leachate and final fluid, after full freezing and thawing is most likely linked to coagulation, precipitation and removal (on filters) in the form of amorphous organic-rich solid phases. Detailed molecular mechanisms of this freeze-induced coagulation of ionic solutes and colloids are not known [31,41,42]. The chemical nature of coagulated material has not been investigated in the present study, but most likely includes, in addition to organic humic particles (e.g., [64]), organo-mineral composites of Fe and Al (hydr)oxides tightly linked to organic matter (OM). Such complex compounds are primary carriers of trace metal in soils and groundwaters [65–67] as also evidenced by studies of colloidal matter in surface waters of permafrost peatlands [8–10,68].

Despite these measurable but rather minor decrease in some component concentration between the initial leachate and final fluid obtained after full freezing and thawing of reactors, the present study evidenced rather good recovery of DOC and most solutes. The results of the present study thus corroborate reported earlier rather minor (i.e., < 10-30 %) effects of freeze-thaw cycles on DOC quantity and quality in peat leachates which indicates strong stability of DOM in acidic surface waters [42]. Overall, this demonstrates high stability of dissolved (< 0.45µm) OC, Fe, Al and some trace metals to repetitive freezing and thawing of surface waters in permafrost peatlands.

Preprints (www.preprints.org) | NOT PEER-REVIEWED | Posted: 13 March 2023 doi:10.20944/preprints202303.0200.v1

5. Conclusions

Experimental modelling of complete freezing and thawing of aqueous leachates of peat originated from permafrost peatlands demonstrated systematic evolution of solute concentration of remaining/forming fluids in the course of progressive freezing/thawing, respectively. The ratio of element concentration in the initial filtrate and the one formed after complete freezing and thawing varied depending on the nature of element and its relative affinity to organic matter, Fe/Al hydroxide colloids or simple ionic complexes. The leachates of frozen peat behaved drastically different from leachates of peat from the active layer, as the concentration of DOC, Fe and other solutes in the remaining fluid did not increase upon progressive freezing. We thus demonstrate efficient incorporation of solutes from frozen peat leachates into the forming ice, as reflected by quite low partitioning coefficients of elements between forming ice and remaining fluid for this type of substrate. We hypothesize that some volumes of the fluid, formed from frozen leachate, partially preserved the peat dispersed ice structure and chemical composition and could be directly incorporated into forming ice with a partitioning coefficient close to 1.

Author Contributions: Conceptualization, I.S.I and O.S.P.; field sampling, I.S.I., L.S.Sh.; analysis of collected samples, J.L.R., I.S.I. and L.S.Sh.; experiments, I.S.I. and O.S.P..; visualization, I.S.I.; writing and editing O.S.P., I.S.I., L.S.Sh. and J.L.R. All authors have read and agreed to the published version of the manuscript.

Funding: The study was funded by the Ministry of Education and Science of the Russian Federation (Agreement No. 075-15-2022-241).

Conflicts of Interest: The authors declare no conflict of interest.

References

1. Henry, H.A.L. Climate change and soil freezing dynamics: historical trends and projected changes. *Clim. Change*. **2008**, 87, 421–434. https://doi.org/10.1007/s10584-007-9322-8.
2. Hayashi, M. The cold vadose zone: Hydrological and ecological significance of frozen-soil processes. *Vadoze Zone J*. **2013**, 12(4), 1–8. https://doi.org/10.2136/vzj2013.03.0064.
3. Fu, Z.; Wu, Q.; Zhang, W.; He, H.; Wang, L. Water migration and segregated ice formation in frozen ground: Current advances and future perspectives. *Front. Earth Sci*. **2022**, 10, 826961.
4. Reeve, A.S.; Siegel, D.I.; Glaser, P.H. Geochemical controls on peatland pore water from the Hudson Bay Lowland: a multivariate statistical approach. *J. Hydrol*. **1996**, 181, 285–304.
5. Raudina, T.V.; Loiko, S.V.; Lim, A.G.; Krickov, I.V.; Shirokova, L.S.; Istigechev, G.I.; Kuzmina, D.M.; Kulizhsky, S.P.; Vorobyev, S.N.; Pokrovsky, O.S. Dissolved organic carbon and major and trace elements in peat porewater of sporadic, discontinuous, and continuous permafrost zones of western Siberia. *Biogeosciences*. **2017**, 14, 3561–3584. https://doi.org/10.5194/bg-14-3561-2017.
6. Ma, Q.; Jin, H.; Yu, C.; Bense, V.F. Dissolved organic carbon in permafrost regions: A review. *Sci. China Earth Sci*. **2019**, 62, 349–364. https://doi.org/10.1007/s11430-018-9309-6.
7. Pokrovsky, O.S.; Manasypov, R.M.; Kopysov, S.G.; Krickov, I.V.; Shirokova, L.S.; Loiko, S.V.; Lim, A.G.; Kolesnichenko, L.G.; Vorobyev, S.N.; Kirpotin, S.N. Impact of permafrost thaw and climate warming on riverine export fluxes of carbon, nutrients and metals in Western Siberia. *Water*. **2020**, 12, 1817. https://doi.org/10.3390/w12061817.
8. Pokrovsky, O.S.; Manasypov, R.M.; Loiko, S.V.; Shirokova, L.S. Organic and organo-mineral colloids in discontinuous permafrost zone. *Geochim. Cosmochim. Acta*. **2016**, 188, 1–20. https://doi.org/10.1016/j.gca.2016.05.035.
9. Lim, A.G.; Loiko, S.V.; Kuzmina, D.M.; Shirokova, L.S.; Pokrovsky, O.S. Organic carbon, and major and trace elements reside in labile low-molecular form in the ground ice of permafrost peatlands: a case study of colloids in peat ice of Western Siberia. *Environ. Sci.: Processes Impacts*. **2022**, 24, 1443–1459, DOI: 10.1039/D1EM00547B.
10. Raudina, T.V.; Loiko, S.V.; Kuzmina, D.M.; Shirokova, L.S.; Kulizhsky, S.P.; Golovatskaya, E.A.; Pokrovsky, O.S. Colloidal organic carbon and trace elements in peat porewaters across a permafrost gradient in Western Siberia. *Geoderma*. **2021**, 390, 114971. https://doi.org/10.1016/j.geoderma.2021.114971.
11. Manasypov, R.M.; Vorobyev, S.N.; Loiko, S.V.; Kritzkov, I.V.; Shirokova, L.S.; Shevchenko, V.P.; Kirpotin, S.N.; Kulizhsky, S.P.; Kolesnichenko, L.G.; Zemtzov, V.A.; Sinkinov, V.V.; Pokrovsky, O.S. Seasonal

dynamics of organic carbon and metals in thermokarst lakes from the discontinuous permafrost zone of western Siberia. *Biogeosciences*. **2015**, 12, 3009–3028.
12. DeLuca, T.H.; Keeney, D.R.; McCarty, G.W. Effect of freeze-thaw events on mineralization of soil nitrogen. *Biol. Fertil. Soils*. **1992**, 14, 116–120. https://doi.org/10.1007/BF00336260.
13. Dietzel, M. Impact of cycling freezing on precipitation of silica in Me-SiO_2-H_2O systems and geochemical implications for cryosoils and sediments. *Chem. Geol*. **2005**, 216, 79–88.
14. Du, L.; Dyck, M.; Shotyk, W.; He, H.; Lv, J.; Cuss, C.; Bie, J. Lead immobilization processes in soils subjected to freeze-thaw cycles. *Ecotoxicol. Environ. Saf.* **2020**,192, 110288.
15. Fitzhugh, R.D.; Driscoll, C.T.; Groffman, P.M.; Tierney, G.L.; Fahey, T.J.; Hardy, J.P. Soil freezing and the acid-base chemistry of soil solutions in a northern hardwood forest. *Soil Sci. Soc. Am. J*. **2003**, 67, 1897–1908.
16. Hentschel, K.; Borken, W.; Matzner, E. Repeated freeze–thaw events affect leaching losses of nitrogen and dissolved organic matter in a forest soil. *J. Plant. Nutr. Soil Sci*. **2008**, 171:699–706. https://doi.org/10.1002/jpln.200700154.
17. Kim, E-A.; Lee, H.K.; Choi, J.H. Effects of a controlled freeze-thaw event on dissolved and colloidal soil organic matter. *Environ. Sci. Pollut. Res*. **2017**, 24, 1338–1346. https://doi.org/10.1007/s11356-016-7552-x.
18. Larsen, K.S.; Jonasson, S.; Michelsen, A. Repeated freeze–thaw cycles and their effects on biological processes in two arctic ecosystem types. *Appl. Soil Ecol*. **2002**, 21, 187–195. https://doi.org/10.1016/S0929-1393(02)00093-8.
19. Leuther, F.; Schlüter, S. Impact of freeze-thaw cycles on soil structure and soil hydraulic properties. *Soil*. **2021**, 7, 179-191.
20. Mohanty, S.K.; Saiers, J.E.; Ryan, J.N. Colloid-facilitated mobilization of metals by freeze-thaw cycles. *Environ. Sci. Technol*. **2014**, 48, 977–984.
21. Mohanty, S.K.; Saiers, J.E.; Ryan, J.N. Colloid mobilization in a fractured soil during dry-wet cycles: Role of drying duration and flow path permeability. *Environ. Sci. Technol*. **2015**, 49, 9100–9106.
22. Ren, J.; Vanapalli, S.K. Effect of freeze–thaw cycling on the soil-freezing characteristic curve of five Canadian soils. *Vadose Zone J*. **2020**, 19, e20039. https://doi.org/10.1002/vzj2.20039.
23. Semenov, V.M.; Kogut, B.M.; Lukin, S.M. Effect of repeated drying-wetting-freezing-thawing cycles on the active soil organic carbon pool. *Eurasian Soil Sci*. **2014**, 47, 276–286.
24. Schimel, J.P.; Clein, J.S. Microbial response to freeze-thaw cycles in tundra and taiga soils. *Soil Biol. Biochem*. **1996**, 28, 1061–1066. https://doi.org/10.1016/0038-0717(96)00083-1.
25. Vestgarden, L.S.; Austnes, K. Effects of freeze–thaw on C and N release from soils below different vegetation in a montane system: a laboratory experiment. *Glob. Change Biol*. **2009**, 15, 876–887. https://doi.org/10.1111/j.1365-2486.2008.01722.x.
26. Xiao, L.; Zhang, Ya.; Li, P.; Xu, G.; Shi, P.; Zhang, Yi. Effects of freeze-thaw cycles on aggregate-associated organic carbon and glomalin-related soil protein in natural-succession grassland and Chinese pine forest on the Loess Plateau. *Geoderma*. **2019**, 334, 1–8. https://doi.org/10.1016/j.geoderma.2018.07.043.
27. Zhang, Z.; Ma, W.; Feng, W.; Xiao, D.; Hou, X. Reconstruction of soil particle composition during freeze-thaw cycling: A review. *Pedosphere*. **2016**, 26, 167–179.
28. Nagare, R.M.; Schincariol, R.A.; Quinton, W.L.; Hayashi, M. Effects of freezing on soil temperature, freezing front propagation and moisture redistribution in peat: laboratory investigations. *Hydrol. Earth. Syst. Sci*. **2012***a*, 16(2), 501–515. https://doi.org/10.5194/hess-16-501-2012.
29. Nagare, R.M.; Schincariol, R.A.; Quinton, W.L.; Hayashi, M. Moving the field into the lab: Simulation of water and heat transport in Subarctic Peat. *Permafrost Periglacial Proc*. **2012***b*, 23(3), 237–243. https://doi.org/10.1002/ppp.1746.
30. Smerdon, B.D.; Mendoza, C.A. Hysteretic freezing characteristics of riparian peatlands in the Western Boreal Forest of Canada. *Hydrol. Process*. **2010**, 24(8), 1027–1038. https://doi.org/10.1002/hyp.7544.
31. McCarter, C.P.R.; Rezanezhad, F.; Quinton, W.L.; Gharedaghloo, B.; Lennartz, B.; Price, J.; Connon, R.; Van Cappellen, P. Pore-scale controls on hydrological and geochemical processes in peat: Implications on interacting processes. *Earth-Sci. Rev*. **2020**, 207,103227. https://doi.org/10.1016/j.earscirev.2020.103227.
32. Schwamborn, G.; Schirrmeister, L.; Frütsch, F.; Diekmann, B. Quartz weathering in freeze–thaw cycles: experiment and application to the El'gygytgyn Crater Lake record for tracing Siberian permafrost history. *Geografiska Annaler: Series A, Physical Geography*. **2012**, 94, 481–499. doi:10.1111/j.1468-0459.2012.00472.x.

33. Wang, J.Y.; Song, C.C.; Hou, A.X.; Miao, Y.Q.; Yang, G.S.; Zhang, J. Effects of freezing thawing cycle on peatland active organic carbon fractions and enzyme activities in the Da Xing'anling Mountains, Northeast China. *Environ. Earth Sci*. **2014**, 72, 1853–1860.
34. Chen, J.; Xue, S.; Lin, Y.; Wang, C.; Wang, Q.; Han, Q. Effect of freezing–thawing on dissolved organic matter in water. *Desalination Water Treat.* **2016**, 57, 17230–17240. https://doi.org/10.1080/19443994.2015.1085913.
35. Fellman, J.B.; D'Amore, D.V.; Hood, E. An evaluation of freezing as a preservation technique for analyzing dissolved organic C, N and P in surface water samples. *Sci. Total. Environ.* **2008**, 392, 305–312. https://doi.org/10.1016/j.scitotenv.2007.11.027.
36. Jiang, N.; Juan, Y.; Tian, L.; Chen, X.; Sun, W.; Chen, L. Modification of the composition of dissolved nitrogen forms, nitrogen transformation processes, and diversity of bacterial communities by freeze–thaw events in temperate soils. *Pedobiologia*. **2018**, 71, 41–49, https://doi.org/10.1016/j.pedobi.2018.08.004.
37. Kim, E-A.; Choi, J.H. Changes in the mineral element compositions of soil colloidal matter caused by a controlled freeze-thaw event. *Geoderma*. **2018**, 318, 160–166. https://doi.org/10.1016/j.geoderma.2017.10.056.
38. Chung, H.Y..; Jung, J.; Lee, D.H.; Kim, S.; Lee, M.K.; Lee, J.I.; Yoo, K.-C.; Lee, Y.I.; Kim. K. Chemical weathering of granite in ice and its implication for weathering in polar regions. *Minerals*. **2020**, 10, 185. https://doi: 10.3390/min10020185.
39. Savenko, A.V.; Savenko, V.S.; Pokrovsky, O.S. Phase fractionation of chemical elements during the formation of ice in fresh surface waters. *Doklady Acad. Sci. Ser. Earth Sci. Geography*. **2020**, 492(1), 48–54. https://doi.org/10.1134/S1028334X20050207.
40. Morgalev, S.Y.; Morgaleva, T.G.; Morgalev, Y.N.; Loiko, S.V.; Manasypov, R.M.; Lim, A.G.; Pokrovsky, O.S. Experimental modeling of the bacterial community translocation during freezing and thawing of peat permafrost soils of Western Siberia. *IOP Conference Series: Earth and Environmental Science*. **2019**, 400(1), 012017. https://doi.org/ 10.1088/1755-1315/400/1/012017.
41. Morgalev, S.Yu.; Lim, A.G.; Morgaleva, T.G.; Morgalev, Yu.N.; Manasypov, R.M.; Kuzmina, D.M.; Shirokova, L.S.; Orgogozo, L.; Loiko, S.V.; Pokrovsky, O.S. Fractionation of organic C, nutrients, metals and bacteria in peat porewater and ice after freezing and thawing. *Environmental Science Pollution Research*. **2023**, 30, 823–836.DOI: 10.1007/s11356-022-22219-1.
42. Payandi-Rolland, D.; Shirokova, L.S.; Labonne, F.; Bénézeth, P.; Pokrovsky, O.S. Low impact of freeze-thaw cycles on organic carbon and metals in waters of permafrost peatlands. *Chemosphere*. **2021**, 279, 130510. https://doi.org/10.1016/j.chemosphere.2021.130510.
43. Shirokova, L.S.; Chupakov, A.V.; Zabelina, S.A.; Neverova, N.V.; Payandi-Rolland, D.; Causseraund, C.; Karlsson, J.; Pokrovsky, O.S. Humic surface waters of frozen peat bogs (permafrost zone) are highly resistant to bio- and photodegradation. *Biogeosciences*. **2019**, 16, 2511–2526.
44. Shirokova, L.S.; Chupakov, A.V.; Ivanova, I.S.; Moreva, O.Y.; Zabelina, S.A.; Shutskiy, N.A.; Loiko, S.V.; Pokrovsky, O.S. Lichen, moss and peat control of C, nutrient and trace metal regime in lakes of permafrost peatlands. *Science Total Environment*. **2021**, 782, 146737. https://doi.org/10.1016/j.scitotenv.2021.146737.
45. Morgalev, Y.N.; Lushchaeva, I.V.; Morgaleva, T.G.; Kolesnichenko, L.G.; Loiko, S.V.; Krickov, I.V.; Lim, A.G.; Raudina, T.V.; Volkova, I.I.; Shirokova, L.S.; Morgalev, S.Y.; Vorobyev, S.N.; Kirpotin, S.N.; Pokrovsky, O.S. Bacteria primarily metabolize at the active layer/permafrost border in the peat core from a permafrost region in western Siberia. *Polar Biol*. **2017**, 40, 1645–1659. https://doi.org/10.1007/s00300-017-2088-1.
46. Aksenov, A.S.; Shirokova, L.S.; Kisil, O.Ya.; Kolesova, S.N.; Lim, A.G.; Kuzmina, D.M.; Pouille, S.; Alexis, M.A.; Castrec-Rouelle, M.; Loiko, S.V.; Pokrovsky, O.S. Bacterial number and genetic diversity in a permafrost peatland (western Siberia): testing a link with organic matter quality and elementary composition of a peat soil profile. *Diversity (MDPI)*. **2021**, 13, 328. https://doi.org/10.3390/d13070328.
47. Heimburger, A.; Tharaud, M.; Monna, F.; Losno, R.; Desboeufs, K.; Nguyen, E. SLRS-5 elemental concentrations deduced from SLRS-5/SLRS-4 ratios of thirty-three uncertified elements. *Geostandards Geoanalyt. Research*. **2013**, 37 (1), 77–85. 10.1111/j.1751-908X.2012.00185.x.
48. Yeghicheyan, D.; Bossy, C.; Bouhnik Le Coz, M.; Douchet, Ch.; Granier, G.; Heimburger, A.; Lacan, F.; Lanzanova, A.; Rousseau, T.C.C.; Seidel, J-L.; Tharaud, M.; Candaudap, F.; Chmeleff, J.; Cloquet, C.; Delpoux, S.; Labatut, M.; Losno, R.; Pradoux, C.; Sivry, Y.; Sonke, J.E. A compilation of silicon, rare earth element and twenty-one other trace element concentrations in the natural river water Reference Material

Preprints (www.preprints.org) | NOT PEER-REVIEWED | Posted: 13 March 2023 doi:10.20944/preprints202303.0200.v1

SLRS-5 (NRC-CNRC). *Geostand. Geoanal. Res*. **2013**, 37, 449–467. https://doi:10.1111/j.1751-908X.2013.00232.x.

49. Pokrovsky, O.S.; Karlsson, J.; Giesler, R. Freeze-thaw cycles of Arctic thaw ponds remove colloidal metals and generate low-molecular-weight organic matter. *Biogeochemistry*. **2018**, 137, 321–336. https://doi.org/10.1007/s10533-018-0421-6.
50. Lim, A.G.; Loiko, S.V.; Kuzmina, D.M.; Krickov, I.V.; Shirokova, L.S.; Kulizhsky, S.P.; Vorobyev, S.N.; Pokrovsky, O.S. Dispersed ground ice of permafrost peatlands: a non-accounted for source of C, nutrients and metals. *Chemosphere*. **2021**, 226, 128953. https://doi.org/10.1016/j.chemosphere.2020.128953.
51. Kokelj, S.V., Burn, C.R. Geochemistry of the active layer and near-surface permafrost, Mackenzie delta region, Northwest Territories, Canada. *Canadian Journal of Earth Sciences*. **2005**, 42, 37–48.
52. French, H.; Shur, Y. The principles of cryostratigraphy. *Earth-Science Reviews*. **2010**, 101, 190–206. https://doi.org/10.1016/j.earscirev.2010.04.002.
53. Lamhonwah, D.; Lafrenière, M.J.; Lamoureux, S.F.; Wolfe, B.B. Multi-year impacts of permafrost disturbance and thermal perturbation on High Arctic stream chemistry. *Arctic Science*. **2016**, 3, 254–276. https://doi.org/10.1139/as-2016-0024.
54. Lamhonwah, D.; Lafrenière, M.J.; Lamoureux, S.F.; Wolfe, B.B. Evaluating the hydrological and hydrochemical responses of a High Arctic catchment during an exceptionally warm summer. *Hydrological Processes*. **2017**, 31, 2296–2313. https://doi.org/10.1002/hyp.11191.
55. Ewing, S.A.; O'Donnell, J.A.; Aiken, G.R.; Butler, K.; Butman, D.; Windham-Myers, L.; Kanevskiy, M.Z. Long-term anoxia and release of ancient, labile carbon upon thaw of Pleistocene permafrost. *Geophys. Res. Lett*. **2015**, 42(2410), 10730–10738.
56. Ostroumov, V.; Hoover, R.; Ostroumova, N.; Van Vliet-Lanoë, B.; Siegert, C.; Sorokovikov, V. Redistribution of soluble components during ice segregation in freezing ground. *Cold Regions Sci. Technol.* **2001**, 32(2), 175–182.
57. Shafique, U.; Anwar, J.; uz-Zaman, W.; Rehman, R.; Salman, M.; Dar, A.; Jamil, N. Forced migration of soluble and suspended materials by freezing front in aqueous systems. *J. Hydro-Environ. Res*. **2012**, 6, 221–226. https://doi.org/10.1016/j.jher.2011.10.001.
58. Takenaka, N.; Bandow, H. Chemical kinetics of reactions in the unfrozen solution of ice. *J. Phys. Chem. A*. **2007**, 111(36), 8780-8786.
59. Elliott, A.C.; Henry, H.A.L. Freeze–thaw cycle amplitude and freezing rate effects on extractable nitrogen in a temperate old field soil. *Biol. Fertil. Soils*. **2009**, 45, 469–476. https://doi.org/10.1007/s00374-009-0356-0.
60. Xue, S.; Wen, Y.; Hui, X.; Zhang, L.; Zhang, Z.; Wang, J.; Zhang, Y. The migration and transformation of dissolved organic matter during the freezing processes of water. *J. Environ Sci*. **2015**, 27, 168–178. https://doi.org/10.1016/j.jes.2014.05.035.
61. Petrich, C.; Eicken, H. Growth, Structure and Properties of Sea Ice. In: *Sea Ice*, 2nd ed.; Thomas, D.N., Dieckmann, G.S., Eds.; Wiley Blackwell: Oxford, UK, **2010**, Volume 2, pp 425–467. https://doi.org/10.1002/9781444317145.ch2.
62. Chen, C.; Huang, H.; Mo, X.; Xue, H.; Liu, M.; Chen, H. Insights into the kinetic processes of solute migration by unidirectional freezing in porous media with micromodel visualization at the pore-scale. *Sci. Total Environ*. **2021**, 784, 147178.
63. Ju, Z.; Du, Z.; Guo, K.; Liu, X. () Irrigation with freezing saline water for 6 years alters salt ion distribution within soil aggregates. *J. Soil Sediments*. **2019**, 19, 97–105.
64. Giesy, J.P.; Briese, L.A. Particulate formation due to freezing humic waters. *Water Resour. Res*. **1978**, 14, 542–544. https://doi.org/10.1029/WR014i003p00542.
65. McCarthy, J.F, Zachara, J.M. Subsurface transport of contaminants. *Environ. Sci Technol*. **1989**, 23, 496–502. https://doi.org/10.1021/es00063a001.
66. Murphy, E.M.; Zachara, J.M. The role of sorbed humic substances on the distribution of organic and inorganic contaminants in groundwater. *Geoderma*. **1995**, 67, 103–124. https://doi.org/10.1016/0016-7061(94)00055-F.

67. Otero Farina, A.; Peacock, C.L.; Fiol, S.; Antelo, J.; Carvin, B. A universal adsorption behaviour for Cu uptake by iron (hydr) oxide organo-mineral composites. *Chem. Geol*. **2018**, 479, 22–35. https://doi.org/10.1016/j.chemgeo.2017.12.022.
68. Krickov, I.V.; Pokrovsky, O.S.; Manasypov, R.M.; Lim, A.G.; Shirokova, L.S.; Viers, J. Colloidal transport of carbon and metals by western Siberian rivers during different seasons across a permafrost gradient. *Geochim. Cosmochim. Acta* **2019**, *265*, 221-241. https://doi.org/10.1016/j.gca.2019.08.041.

Disclaimer/Publisher's Note: The statements, opinions and data contained in all publications are solely those of the individual author(s) and contributor(s) and not of MDPI and/or the editor(s). MDPI and/or the editor(s) disclaim responsibility for any injury to people or property resulting from any ideas, methods, instructions or products referred to in the content.